Twenty Second Annual Conference of the Canadian Nuclear Society
Toronto, Ontario, Canada. June 10-13, 2001

Validation of DRAGON End-Flux Peaking and Analysis of End-Power-Peaking Factors for 37-Element, CANFLEX, and Next-Generation CANDU Fuels

Wei Shen
Atomic Energy of Canada Limited
2251 Speakman Drive
Mississauga, Ontario L5K 1B2
shenwei@aecl.ca

ABSTRACT

Within the framework of adopting WIMS-AECL as the standard lattice-cell code for CANDU® analysis, it is imperative that a methodology compatible with this code be implemented for modelling CANDU bundle end regions in three dimensions. The work reported here had two objectives. First, the DRAGON-calculated end-flux-peaking factors were validated by comparison with measurements for cold fresh 37-element natural-uranium (NU) Bruce-type fuel bundles in the ZED-2 reactor. The validation exercise showed excellent results, with the DRAGON end-flux-peaking factor underestimating the measured value by ~1% for any fuel ring. Second, the end-power-peaking factors were calculated with DRAGON for 37-element, CANFLEX®, and next-generation CANDU fuels at full-power operating conditions.

1. INTRODUCTION

A CANDU fuel channel contains 12 fuel bundles, each measuring ~50 cm in length. The region separating the fuel in two adjoining bundles in a channel is called the "end region"; typically, this is taken as the last 1 to 2 cm at each end of a bundle. The end of the last UO_2 pellet in the fuel stack adjacent to the end region is called the "fuel end". The representation of the CANDU fuel bundle (Figure 1) shows the end region and the fuel-stack length compared with the bundle length. The thermal neutron flux is higher in the end region of the bundle than at the axial mid-point, because of the gap between bundles and because the end region of the bundle is made up of very-low-neutron-absorption material, such as Zircaloy-4 and coolant. The thermal flux also peaks during refuelling at the free end of the last-inserted fresh bundle when the entire fuel-bundle string is temporarily shifted toward the downstream end of the channel. This bundle-coolant contact configuration results in a greater thermal flux peak than that in the normal bundle-bundle contact configuration, although it lasts for only a short period of time (usually about 10 min) and occurs in fresh bundles.

The end-flux peaking leads to a higher fission rate, and hence higher heat production and higher temperatures in the end region of the fuel bundle. For accurate evaluation of fuel performance, it is important to have the capability to accurately calculate the three-dimensional (3D) spatial power distribution in the fuel bundle, including the end region.

Previous calculations of the end-peaking factors were performed in two dimensions (2D) (*R-Z* geometry) with the neutron-transport code PEAKAN[1]. In this paper, the DRAGON[3] code was used

CANDU® is a registered trademark of Atomic Energy of Canada Limited (AECL).
CANFLEX® is a registered trademark of AECL and the Korea Atomic Energy Research Institute (KAERI).

because it has been selected as an Industry Standard Toolset (IST) code. DRAGON's multigroup neutron-transport method is theoretically rigorous and consistent with WIMS-AECL lattice-cell calculations, and allows a good geometrical representation of the CANDU bundle end regions in 3 dimensions.

The work reported here had two objectives. First, the DRAGON-calculated end-flux-peaking factors were validated by comparison with measurements[4] for cold fresh 37-element natural-uranium (NU) Bruce-type fuel bundles in the ZED-2 reactor. The validation exercise showed excellent results, with the DRAGON end-flux-peaking factor underestimating the measured value by ~1% for any fuel ring. Second, the end-power-peaking factors were calculated with DRAGON for fresh 37-element NU fuel and CANFLEX-NU fuel in a CANDU 6 reactor, and for CANFLEX slightly-enriched-uranium (SEU) fuel in a next-generation (NG) CANDU reactor[5].

2. DEFINITION OF PEAKING FACTORS

To better understand the results and discussions shown in the next sections, we first recall the definition of end-peaking factors.

End-flux-peaking factors are defined as:

$$PF_i^{flux} = \frac{\phi_i^{end}}{\phi_i^{mid-plane}}, \quad i = 1, 2, 3, 4 \tag{1}$$

where:

PF_i^{flux}	=	end-flux-peaking factor in element ring *i* (i = 1, 2, 3, 4)
ϕ_i^{end}	=	fuel-end thermal flux in element ring *i* (i = 1, 2, 3, 4), $cm^{-2}\cdot s^{-1}$
$\phi_i^{mid-plane}$	=	local thermal flux in element ring *i* (i = 1, 2, 3, 4) at the bundle mid-plane, $cm^{-2}\cdot s^{-1}$

Two definitions can be used for end-power-peaking factors, *PF*1 and *PF*2:

$$PF1_i^{power} = \frac{P_i^{end}}{P_i^{mid-plane}}, i = 1, 2, 3, 4 \tag{2}$$

$$PF2_i^{power} = \frac{P_i^{end}}{\overline{P}_{bundle}}, i = 1, 2, 3, 4 \tag{3}$$

where:

$PF1_i^{power}$	=	ratio of the fuel-end linear power to the local linear power at the bundle mid-plane in the same element ring *i*
$PF2_i^{power}$	=	ratio of the fuel-end linear power in element ring i to the bundle-average linear power
P_i^{end}	=	fuel-end linear power in element ring *i* (i = 1, 2, 3, 4), W/cm
$P_i^{mid-plane}$	=	local linear power in element ring *i* (i = 1, 2, 3, 4) at the bundle mid-plane, W/cm
$\overline{P}_{bundle}$	=	bundle-average linear power, W/cm

$PF2_i^{power}$ is recommended for use because it is straightforward from the reactor-safety point of view in estimating the maximum linear power and its location. However, it is easy to relate $PF1_i^{power}$ to $PF2_i^{power}$ using the following equations:

$$PF2_i^{power} = PF1_i^{power} NP_i^{mid-plane}, i = 1, 2, 3, 4 \quad (4)$$

$$NP_i^{mid-plane} = \frac{P_i^{mid-plane}}{\overline{P}_{bundle}}, i = 1, 2, 3, 4 \quad (5)$$

where

$NP_i^{mid-plane}$ = the normalized local linear power in element ring *i* (i = 1, 2, 3, 4) at the bundle mid-plane, W/cm

That is to say, the use of $PF1_i^{power}$ is equivalent to that of $PF2_i^{power}$ for safety analysis, as long as $NP_i^{mid-plane}$ distributions are provided as additional parameters.

3. DRAGON THREE-DIMENSIONAL END-REGION MODEL

The DRAGON neutron-transport code was designed for general geometry and can analyze both CANDU clusters and pressurized-water reactor (PWR) assemblies in 2 dimensions, with critical buckling search. The code can also perform 3D supercell transport calculations with the same group structures as those used in 2D analysis. In this study, the DRAGON code was used to perform neutron-transport calculations in a 3D supercell to compute the end-peaking factors. Compared with the previously used PEAKAN end-region model, the DRAGON model used in this study has the following advantages and is expected to produce more reliable predictions of the end-peaking factors:

- consistent 2D cell and 3D supercell methodology with one DRAGON calculation only (WIMS-AECL calculation had to be performed to generate cross-section data for the PEAKAN analysis);
- three-dimensional *X-Y-Z* and *R-Z* geometry used in DRAGON (2D *R-Z* geometry used in PEAKAN);
- 89-group transport calculation performed in DRAGON (only 2- or 4-group transport calculation was done with PEAKAN);
- no boundary condition imposed in the end region or the bundle mid-plane for DRAGON analysis (boundary condition is used in the end region for PEAKAN analysis);
- longer axial length (1 bundle or 3 bundles long) used in DRAGON;
- finer axial mesh-spacing design (70 or 100 axial meshes) used in DRAGON.

All the calculations reported in this paper were performed using the DRAGON code (version 3.03a, released as DRAGON981110) with its latest 89-group ENDF/B-V library. The current standard ENDF/B-VI library was not used in this study because it is still unavailable in a format that the DRAGON code can use. In this paper, a DRAGON end-region model was set up to model various fuel-bundle types (37-element NU, CANFLEX-NU, and NG CANDU CANFLEX-SEU fuels), at full power, for both bundle-bundle contact and bundle-coolant contact.

The Point Lepreau Generating Station (PLGS) ZTFU02 fuel type and the as-built CANFLEX-NU fuel used in the Point-Lepreau reactor for the demonstration irradiation were chosen as the reference 37-element and CANFLEX-NU fuels in this analysis, respectively.

The typical NG CANDU CANFLEX-SEU lattice, as shown in Figure 2, contains a 43-element CANFLEX bundle and pressurized light-water coolant in a pressure tube enclosed within a calandria tube. Surrounding this calandria tube, a region of unpressurized heavy water at low temperature serves as moderator. Compared with the normal CNADU fuel lattice, the NG CANDU CANFLEX-SEU lattice is cooled with light water and has a smaller lattice pitch and a larger gap between the pressure and calandria tubes. The enrichment of the NG CANDU CANFLEX-SEU fuel used in this analysis is about 1.5 wt%.

Figures 3 and 4 show the *X*-*Z* layout (right-half only) of the 3D DRAGON supercells for 37-element fuel, in bundle-bundle contact and bundle-coolant contact configurations, respectively. The supercell used for bundle-bundle contact configuration is of dimensions 1 lattice pitch x 1 lattice pitch in the *X* and *Y* directions, respectively, and its dimension in the *Z* direction is more than 1 bundle length (about 70 cm long); the supercell used for bundle-coolant contact configuration is of dimensions 1 lattice pitch x 1 lattice pitch x 3 bundle lengths in the *X*, *Y* and *Z* directions. The isotropic reflective boundary conditions were applied in the external surfaces of the supercell model, with symmetry boundary conditions imposed at the surfaces with dotted lines, as shown in Figures 3 and 4. To obtain reliable axial flux distributions, fine axial meshes are imposed in the *Z* direction. The selection of the supercell size and the mesh spacing is a compromise between precision and memory allowance. The supercells for CANFLEX-NU and NG CANDU CANFLEX-SEU fuels are not illustrated here because they are basically the same as those for 37-element fuel, except for the radial dimensions, axial meshes, and material properties, etc.

Isotropic reflective tracking was performed with the 3D collision-probability module EXCELL of DRAGON. The transport equation was solved with a critical buckling search using the homogeneous B1 leakage method. Fuel depletion was not performed in DRAGON, since only fresh fuel bundles were analyzed. After the transport calculation of the 89-energy-group spatial flux distribution, a multi-region homogenization was performed to generate an ASCII file database in which the 2-group neutron flux, 2-group macroscopic cross sections, and volume of each fuel region were saved. From this ASCII file database, the end-peaking factors can be generated.

4. RESULTS AND DISCUSSIONS

4.1 Validation of Dragon End-Flux-Peaking Factors

To evaluate the accuracy of the DRAGON 3D end-region model described above, DRAGON-calculated end-flux-peaking factors were compared with measurements. Measurements of the end-flux-peaking factors were made in the ZED-2 reactor for cold clean fresh 37-element NU Bruce-type fuel bundles in bundle-bundle contact configuration. End-flux-peaking factors and axial flux profiles were measured in representative elements throughout the cluster. A detailed description of the experiments can be found in Reference 4.

The DRAGON-derived end-flux-peaking factors and radial thermal flux distributions at the bundle mid-plane are summarized in Table 1. The measured and PEAKAN-calculated values are listed in Table 1 for comparison. The validation exercise showed excellent results, with the DRAGON end-flux-peaking factor underestimating the measured value by 0.9%, 0.8%, 0.9%, and 1.3% for the centre pin, inner ring, intermediate ring, and outer ring, respectively.

4.2 Calculation of End-Power-Peaking Factors

In Tables 2 and 3, the two different fuel-end power-peaking factors, defined in Equations (2) and (3), and absolute local linear power at the fuel-end and mid-plane of the fuel bundle, are summarized for fresh 37-element, CANFLEX-NU, and NG CANDU CANFLEX-SEU fuels, in bundle-bundle contact

and bundle-coolant contact configurations, respectively. As explained in Section 2, multiplying by the normalized radial pin-power distributions $NP_i^{mid-plane}$ listed in the fourth column of each table, $PF1_i^{power}$ can be easily converted to $PF2_i^{power}$. Although the maximum $PF1_i^{power}$ always appears in the centre ring (pin), the maximum $PF2_i^{power}$ may be in another ring, depending on the radial pin-power distributions. The corresponding axial linear power profiles are plotted in Figures 5, 6, 7, 8, 9 and 10 for fresh 37-element NU, CANFLEX-NU, and NG CANDU CANFLEX-SEU fuels, in bundle-bundle contact and bundle-coolant contact configurations, respectively.

Fresh 37-Element NU Fuel, Bundle-Bundle Contact

Although the maximum $PF1_i^{power}$ is 1.227 in the centre pin, the maximum $PF2_i^{power}$ is found to be 1.252 in the outer ring because the radial linear power peaks in the outer ring and decreases radially toward the centre, as shown in Figure 5. This implies that if the nominal design bundle power is 800 kW, the maximum linear power will be 56.3 kW/m, located at the end of the fuel in the outer ring.

Fresh 37-Element NU Fuel, Bundle-Coolant Contact

In this case, the maximum $PF2_i^{power}$ is 1.445, i.e., about 15% higher than the value in bundle-bundle contact configuration (1.252). As shown in Figure 6, the maximum $PF2_i^{power}$ is also located in the outer ring because the calculated radial linear pin-power distributions are almost unchanged for 37-element fuel operated in different configurations. This implies that if the nominal design bundle power is 800 kW, the maximum linear power in the fuel-end region will consequently be higher than that for bundle-bundle contact configuration by about 15%, 65.0 kW/m compared to 56.3 kW/m.

Fresh CANFLEX-NU Fuel, Bundle-Bundle Contact

In this case, the maximum $PF2_i^{power}$ is 1.271, i.e., about 1.5% higher than the value for 37-element fuel in bundle-bundle contact configuration (1.252). As shown in Figure 7, the maximum $PF2_i^{power}$ switches to the inner ring since the radial linear power peaks in the inner ring because of the larger number pins (43) and the use of thinner pins in the outer two rings in CANFLEX. For a bundle with the nominal design power of 800 kW, these differences result in a maximum element linear power in CANFLEX-NU fuel, relative to the 37-element design, lower by about 13% (49.1 kW/m vs. 56.3 kW/m) at the fuel end, and lower by 19% (40.9 kW/m vs. 50.5 kW/m) at the axial mid-plane.

Fresh CANFLEX-NU Fuel, Bundle-Coolant Contact

In this case, the maximum $PF2_i^{power}$ is 1.613, i.e., about 27% higher than the value for CANFLEX-NU fuel in bundle-bundle contact configuration (1.271). The maximum $PF2_i^{power}$ is also located in the inner ring because the calculated radial linear pin-power distributions are almost unchanged for CANFLEX-NU fuels in bundle-bundle contact configuration, as shown in Figure 8. This implies that if the nominal design bundle power is 800 kW, the maximum linear power in the fuel-end region will consequently be higher than that for CANFLEX-NU fuel in bundle-bundle contact configuration by about 27%, 62.3 kW/m compared to 49.1 kW/m.

NG CANDU CANFLEX-SEU Fuel, Bundle-Bundle Contact

The axial linear power profile for NG CANDU CANFLEX-SEU fuel in bundle-bundle contact configuration is shown in Figure 9. Compared with 37-element fuel in bundle-bundle contact configuration, the maximum $PF2_i^{power}$ is also located in the outer ring, and its value is 1.312, i.e., about 5% higher than the value for 37-element fuel in bundle-bundle contact configuration (1.252). However, the maximum linear power is still lower in NG CANDU CANFLEX-SEU fuel than in 37-element fuel because of the 43-element fuel-bundle design used for NG CANDU CANFLEX-SEU fuel. If the nominal design bundle power is 800 kW, the maximum linear power in the fuel-end region is smaller than that for 37-element fuel in bundle-bundle contact configuration by about 10%, 50.6 kW/m compared to 56.3 kW/m.

NG CANDU CANFLEX-SEU Fuel, Bundle-Coolant Contact

For NG CANDU CANFLEX-SEU fuel, the axial linear power profile, shown in Figure 10, differs significantly from that of 37-element NU fuel. For NG CANDU CANFLEX-SEU fuel, the axial linear power distribution is flat only in the regions close to the bundle mid-plane. Because of the presence of a large amount of light-water coolant near the fuel-bundle end, the linear powers gradually decrease along the axial direction up to about 6 cm away from the fuel end, and then increase quickly in the regions near the fuel end. Compared with 37-element fuel in bundle-coolant contact configuration, the maximum $PF2_i^{power}$ switches from the outer ring to the inner ring, and its value is 1.415, i.e., about 2% smaller than the value for 37-element fuel in bundle-coolant contact configuration (1.445). This value implies that, if the nominal design bundle power is 800 kW, the maximum linear power in the fuel-end region is smaller than that for 37-element fuel in bundle-coolant contact configuration by about 16%, 54.6 kW/m compared to 65.0 kW/m.

5. CONCLUSIONS

The DRAGON end-region model and results were validated by comparison with measurements for cold fresh 37-element NU Bruce-type fuel bundles in the ZED-2 reactor. The validation exercise showed excellent results, with the DRAGON end-flux-peaking factor underestimating the measured value by ~1% for any fuel ring when a fine axial mesh-spacing was used.

The same DRAGON end-region model was used to calculate end-peaking factors for fresh 37-element NU fuel, CANFLEX-NU fuel, and NG CANDU CANFLEX-SEU fuel. For a reference bundle power of 800 kW, the corresponding maximum element linear power at the fuel end was found to be:

- 56.3 kW/m for fresh 37-element NU fuel, in bundle-bundle contact configuration (outer ring)
- 65.0 kW/m for fresh 37-element NU fuel, in bundle-coolant contact configuration (outer ring)
- 49.1 kW/m for fresh CANFLEX-NU fuel, in bundle-bundle contact configuration (inner ring)
- 62.3 kW/m for fresh CANFLEX-NU fuel, in bundle-coolant contact configuration (inner ring)
- 50.6 kW/m for fresh NG CANDU CANFLEX-SEU fuel, in bundle-bundle contact configuration (outer ring)
- 54.6 kW/m for fresh NG CANDU CANFLEX-SEU fuel, in bundle-coolant contact configuration (inner ring)

These results show that, for the same operating conditions, the maximum element linear power at the fuel end is lower in fresh CANFLEX-NU fuel or NG CANDU CANFLEX-SEU fuel than it is in fresh 37-element NU fuel, because of the 43-element design in CANFLEX fuel.

For fresh 37-element NU fuel and CANFLEX-NU fuel, the maximum linear power at the fuel end is ~20% higher in the bundle-coolant contact configuration than in the bundle-bundle contact configuration. In contrast, for fresh CANFLEX-SEU fuel in a NG CANDU reactor, the light-water coolant makes the maximum linear power at the fuel end in the bundle-coolant contact configuration to be only 8% higher than that in the bundle-bundle contact configuration.

It should be noted that all the calculations were performed for fresh fuel because the most severe power peaking happens during the refuelling transient when the coolant contacts the free end of the last-inserted bundle with fresh fuel or slightly irradiated fuel. The DRAGON prediction has been validated to be within an uncertainty of 1.3% for 37-element fuel. There is no reason to expect that this margin of uncertainty would be degraded in CANFLEX fuel.

ACKNOWLEDGEMENTS

The DRAGON code was developed and is maintained at the Institut de Génie Nucléaire, École Polytechnique de Montréal. The author would like to express special thanks to Guy Marleau for his continuous advice and valuable suggestions about DRAGON end-region modelling. The author is also grateful to J.V. Donnelly, H. Chow, D.A. Jenkins, M. Tayal, and Z. Xu for useful technical discussions.

REFERENCES

1. M.H.M. Roshd and H.C. Chow, “The Analysis of Flux Peaking at Nuclear Fuel Bundle Ends Using PEAKAN”, AECL Report, AECL-6174, 1978.
2. J.V. Donnelly, “WIMS-CRNL: A User’s Manual for the Chalk River Version of WIMS”, AECL Report, AECL-8955, 1986.
3. G. Marleau, A. Hébert and R. Roy, “A User’s Guide for DRAGON”, Report IGE-174 Rev 3, École Polytechnique de Montréal, 1998.
4. P.M. French, “Measurements of Bundle End Flux Peaking Effects in 37-Element CANDU PHW Fuel”, AECL Report, AECL-5968, 1977.
5. W. Shen, K. Tsang, and D.B. Buss, “Reactor Physics of NG CANDU”, presented in 22nd Annual Conference of the CNS, Toronto, Canada, June 10-13, 2001.

Table 1: Comparison of Calculated and Measured End-Flux-Peaking Factors for Cold Fresh 37-Element NU Bruce-Type Fuel, in Bundle-Bundle Contact Configuration

Element Ring	End-Flux-Peaking Factors (PF_i^{flux})		
	DRAGON	PEAKAN	Measured Value
Centre	1.257 (-0.9)	1.28 (0.9)	1.268
Inner	1.236 (-0.8)	1.23 (-1.3)	1.246
Intermediate	1.194 (-0.9)	1.20 (-0.4)	1.205
Outer	1.127 (-1.3)	1.13 (-1.1)	1.142

Note: Number in parentheses ( ) refers to percentage error compared with measurement

Table 2: DRAGON-Calculated End-Power-Peaking Factors and Local Linear Powers for Different Fuel Bundles (Bundle-Bundle Contact)

Fresh 37-element NU fuel

Element Ring	End-Power Peaking $PF1_i^{power}$	$PF2_i^{power}$	Local Linear Power at Mid-Plane ($NP_i^{mid-plane}$)	Local Linear Power (kW/m) Fuel-End	Mid-Plane
Centre	1.227	0.919	0.749	41.3	33.7
Inner	1.213	0.954	0.786	42.9	35.3
Intermediate	1.176	1.059	0.899	47.6	40.4
Outer	1.114	1.252	1.124	56.3	50.5

Fresh CANFLEX-NU fuel

Element Ring	End-Power Peaking $PF1_i^{power}$	$PF2_i^{power}$	Local Linear Power at Mid-Plane ($NP_i^{mid-plane}$)	Local Linear Power (kW/m) Fuel-End	Mid-Plane
Centre	1.212	1.189	0.981	45.9	37.9
Inner	1.199	1.271	1.060	49.1	40.9
Intermediate	1.162	0.994	0.855	38.4	33.0
Outer	1.105	1.163	1.052	44.9	40.6

Fresh NG CANDU CANFLEX-SEU fuel

Element Ring	End-Power Peaking $PF1_i^{power}$	$PF2_i^{power}$	Local Linear Power at Mid-Plane ($NP_i^{mid-plane}$)	Local Linear Power (kW/m) Fuel-End	Mid-Plane
Centre	1.333	1.104	0.828	42.6	32.0
Inner	1.317	1.221	0.927	47.1	35.8
Intermediate	1.251	1.036	0.829	40.0	32.0
Outer	1.179	1.312	1.114	50.6	43.0

Note:

1) $PF1_i^{power}$, $PF2_i^{power}$, and $NP_i^{mid-plane}$ are defined in Equations (2), (3), and (5), respectively.
2) Nominal design bundle power is assumed as 800 kW

Table 3: DRAGON-Calculated End-Power-Peaking Factors and Local Linear Powers for Different Fuel Bundles (Bundle-Coolant Contact)

Fresh 37-element NU fuel

Element Ring	End-Power Peaking $PF1_i^{power}$	$PF2_i^{power}$	Local Linear Power at Mid-Plane ($NP_i^{mid-plane}$)	Local Linear Power (kW/m) Fuel-End	Mid-Plane
Centre	1.634	1.182	0.724	53.1	32.5
Inner	1.590	1.206	0.759	54.2	34.1
Intermediate	1.483	1.287	0.868	57.9	39.0
Outer	1.332	1.445	1.085	65.0	48.8

Fresh CANFLEX-NU fuel

Element Ring	End-Power Peaking $PF1_i^{power}$	$PF2_i^{power}$	Local Linear Power at Mid-Plane ($NP_i^{mid-plane}$)	Local Linear Power (kW/m) Fuel-End	Mid-Plane
Centre	1.622	1.538	0.948	59.4	36.6
Inner	1.578	1.613	1.023	62.3	39.5
Intermediate	1.464	1.206	0.824	46.6	31.8
Outer	1.323	1.343	1.015	51.8	39.2

Fresh NG CANDU CANFLEX-SEU fuel

Element Ring	End-Power Peaking $PF1_i^{power}$	$PF2_i^{power}$	Local Linear Power at Mid-Plane ($NP_i^{mid-plane}$)	Local Linear Power (kW/m) Fuel-End	Mid-Plane
Centre	1.514	1.309	0.864	50.5	33.4
Inner	1.466	1.415	0.965	54.6	37.2
Intermediate	1.318	1.136	0.861	43.8	33.2
Outer	1.180	1.362	1.154	52.6	44.5

Note:

3) $PF1_i^{power}$, $PF2_i^{power}$, and $NP_i^{mid-plane}$ are defined in Equations (2), (3), and (5), respectively.

4) Nominal design bundle power is assumed as 800 kW

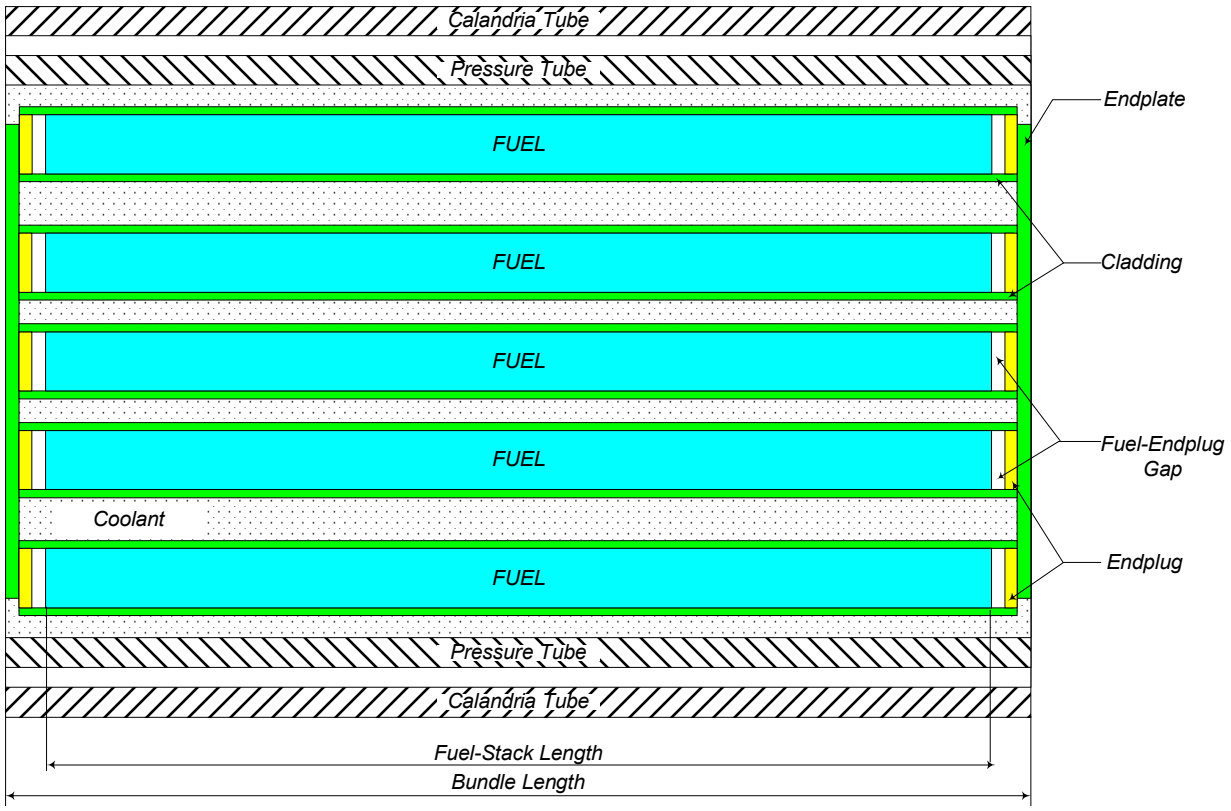

Figure 1: Schematic Representation of a CANDU Fuel Bundle

CANFLEX-NU Fuel Lattice

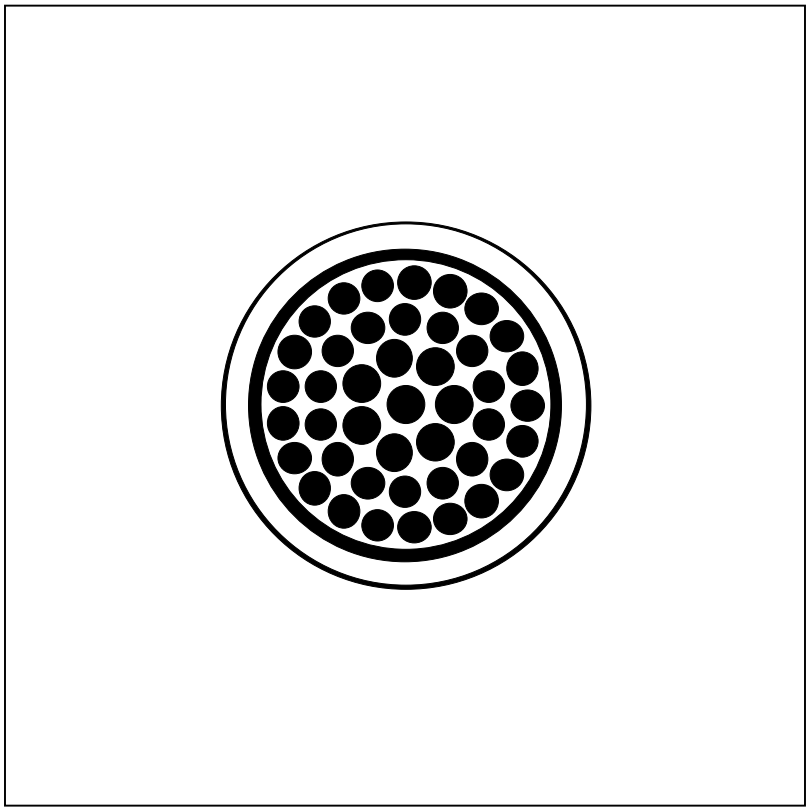

BACK

NG CANDU SEU Fuel Lattice

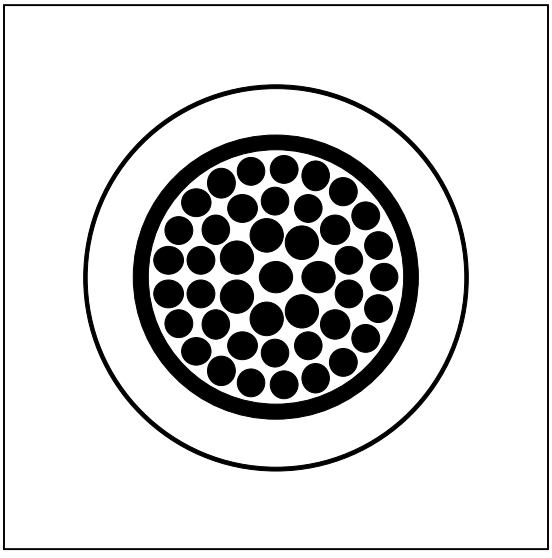

Figure 2: Comparison Between the CANFLEX-NU Fuel Lattice and the NG CANDU CANFLEX-SEU Fuel Lattice

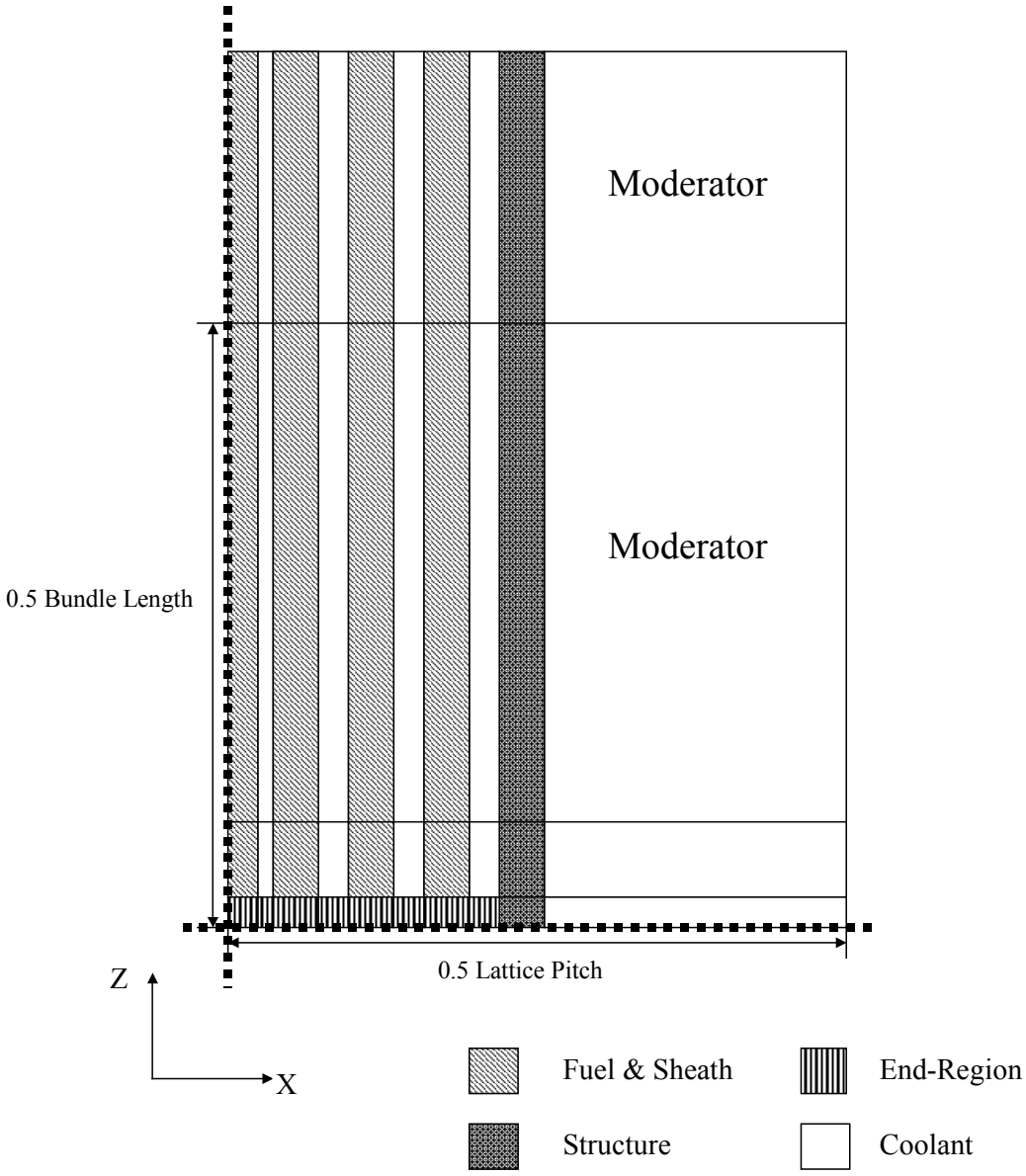

Figure 3: Supercell Modelling of End Region for 37-Element NU fuel, in Bundle-Bundle Contact Configuration (*X-Z* Layout, Right-half Only)

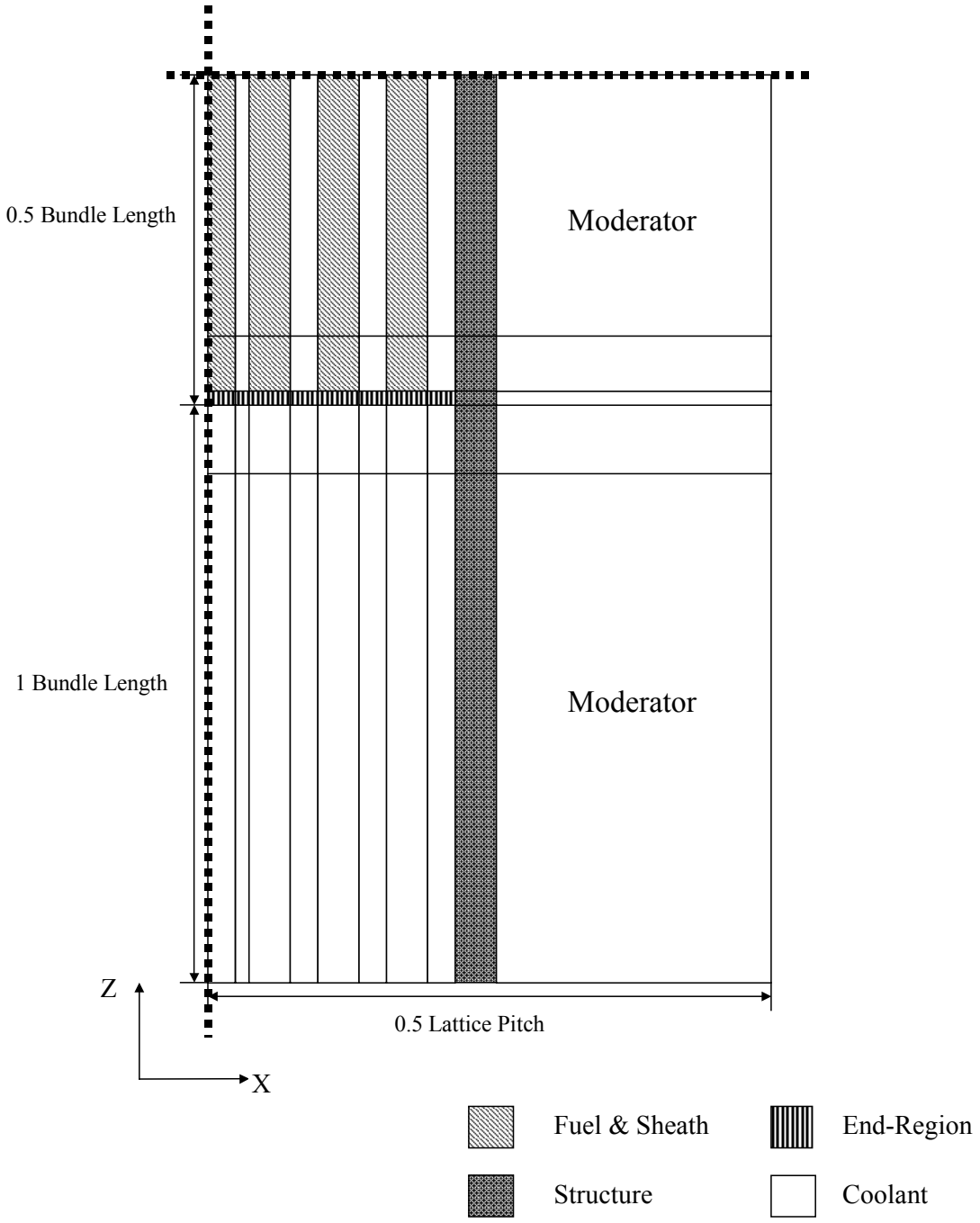

Figure 4: Supercell Modelling of End Region for 37-Element NU Fuel, in Bundle-Coolant Contact Configuration (*X-Z* Layout, Right-half Only)

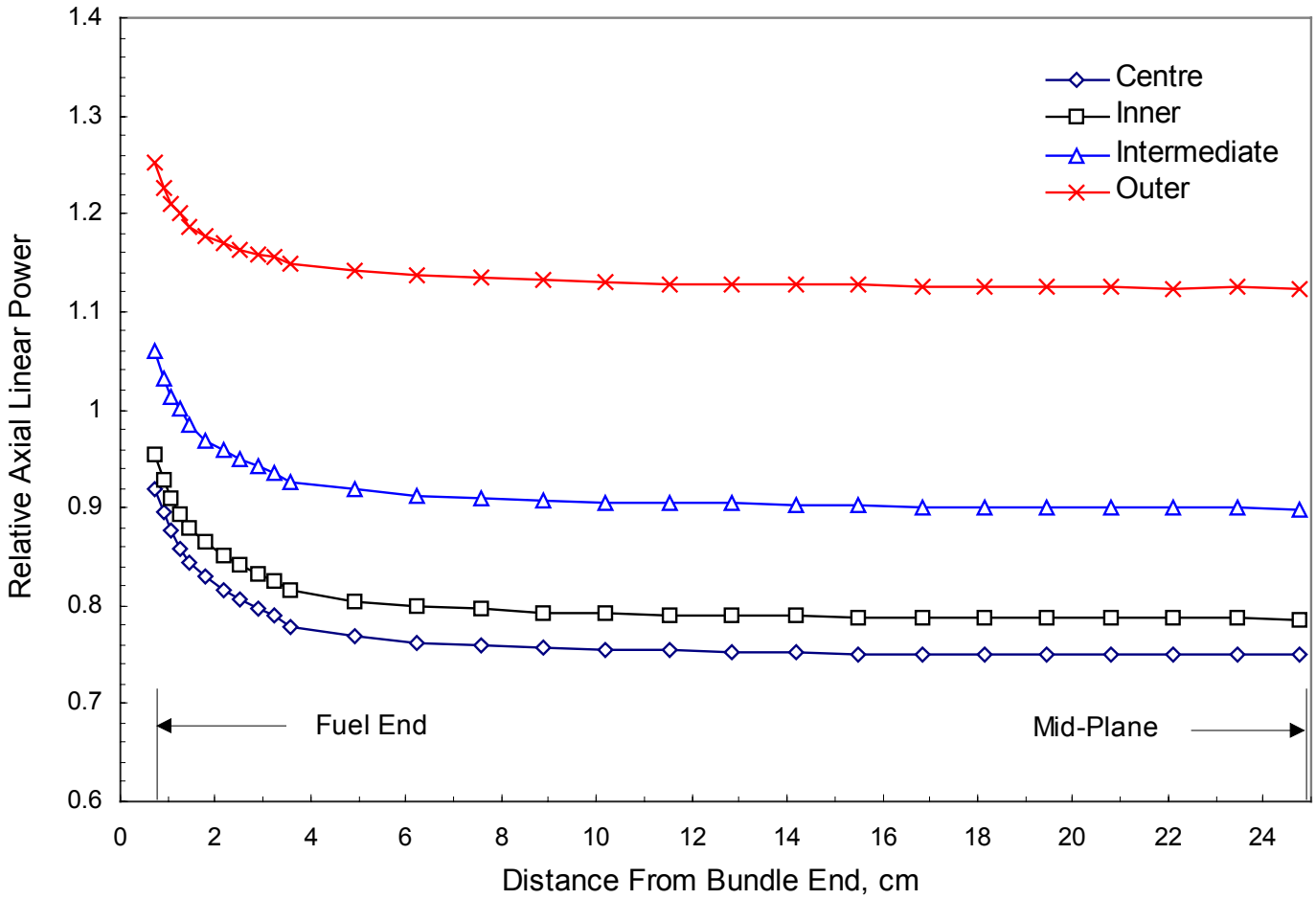

Figure 5: Relative Axial Linear Power Profile for Fresh 37-Element NU Fuel, in Bundle-Bundle Contact Configuration (Bundle-Average Linear Power is Normalized to 1.0)

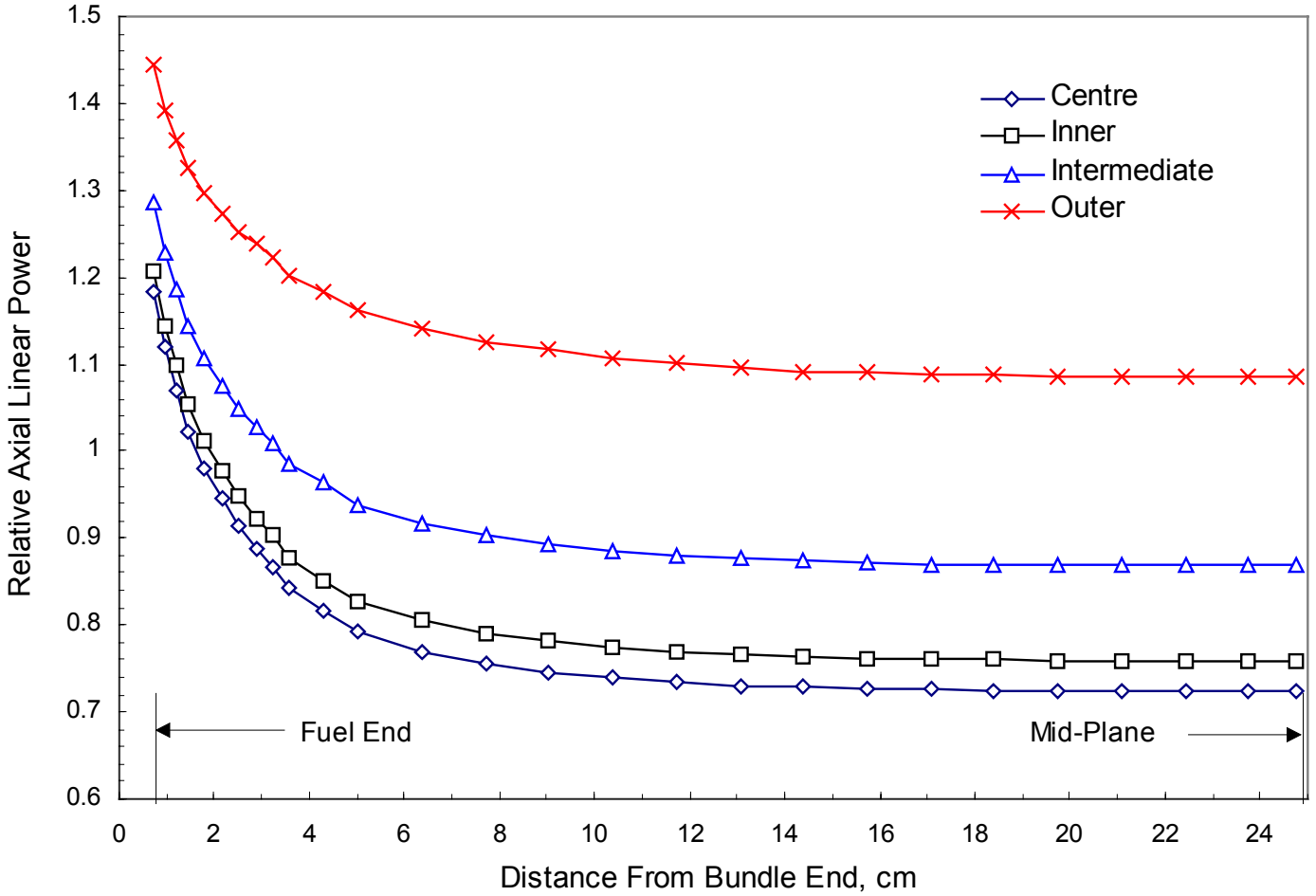

Figure 6: Relative Axial Linear Power Profile for Fresh 37-Element NU Fuel, in Bundle-Coolant Contact Configuration (Bundle-Average Linear Power is Normalized to 1.0)

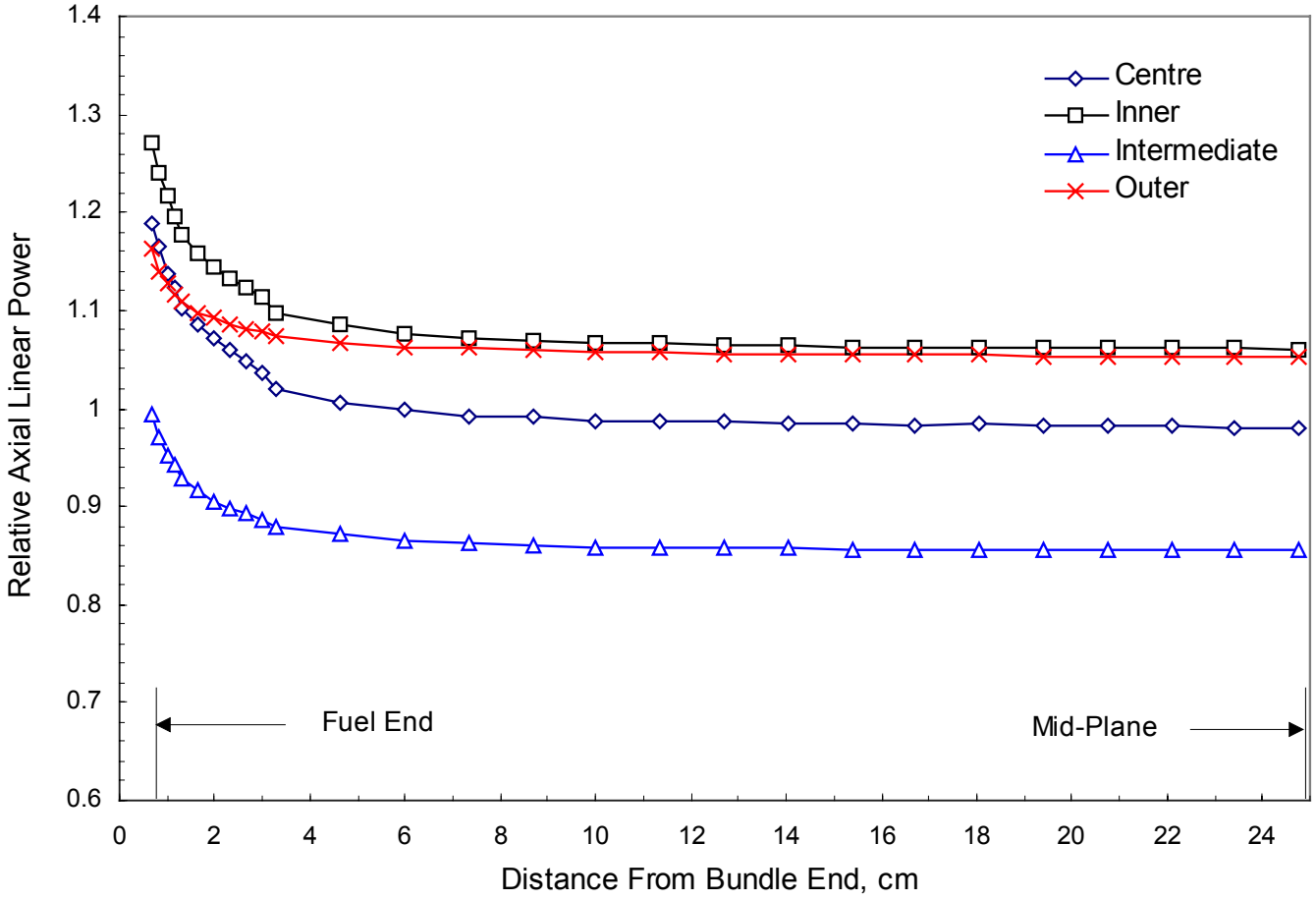

Figure 7: Relative Axial Linear Power Profile for Fresh CANFLEX-NU Fuel, in Bundle-Bundle Contact Configuration (Bundle-Average Linear Power is Normalized to 1.0)

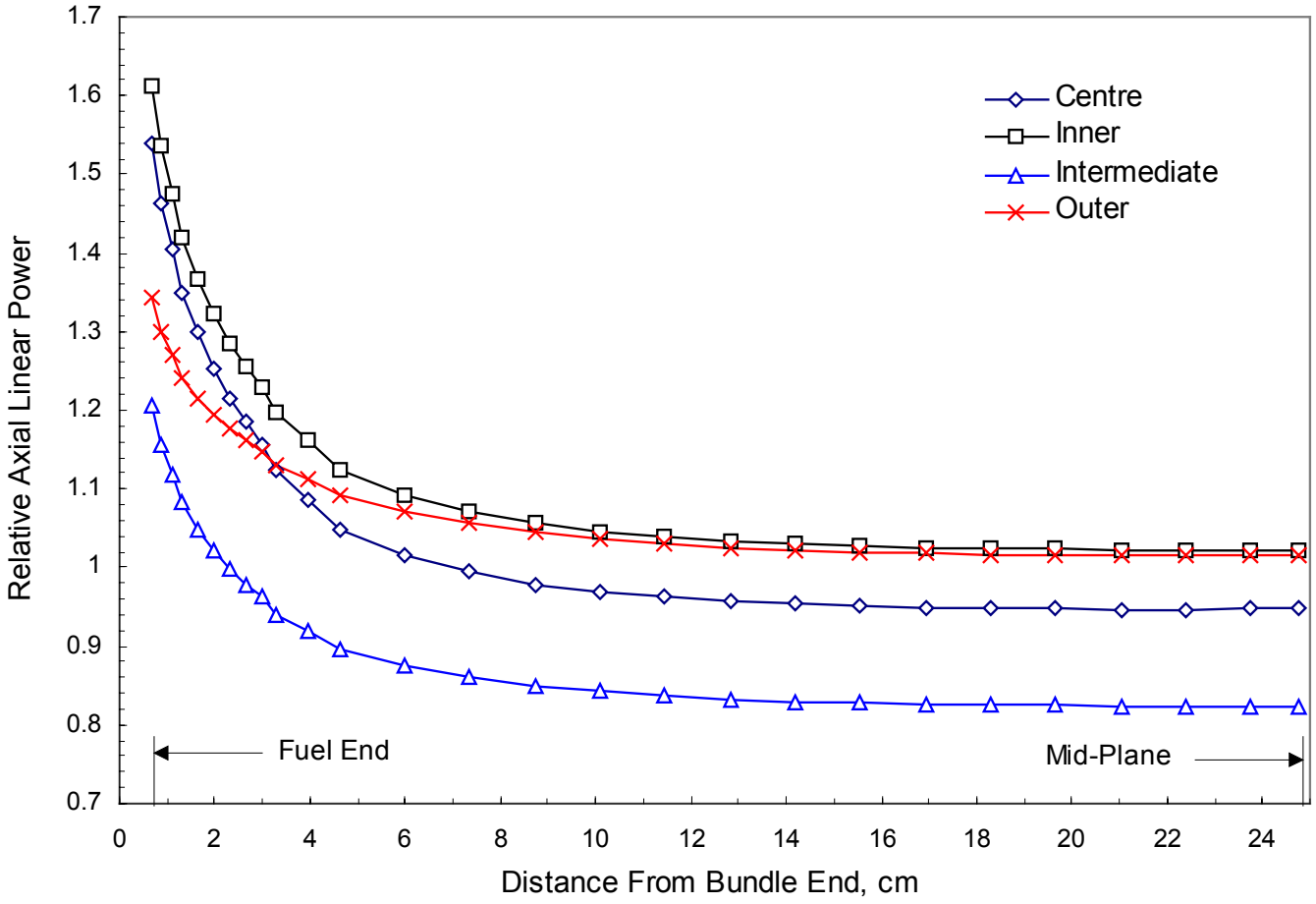

Figure 8: Relative Axial Linear Power Profile for Fresh CANFLEX-NU Fuel, in Bundle-Coolant Contact Configuration (Bundle-Average Linear Power is Normalized to 1.0)

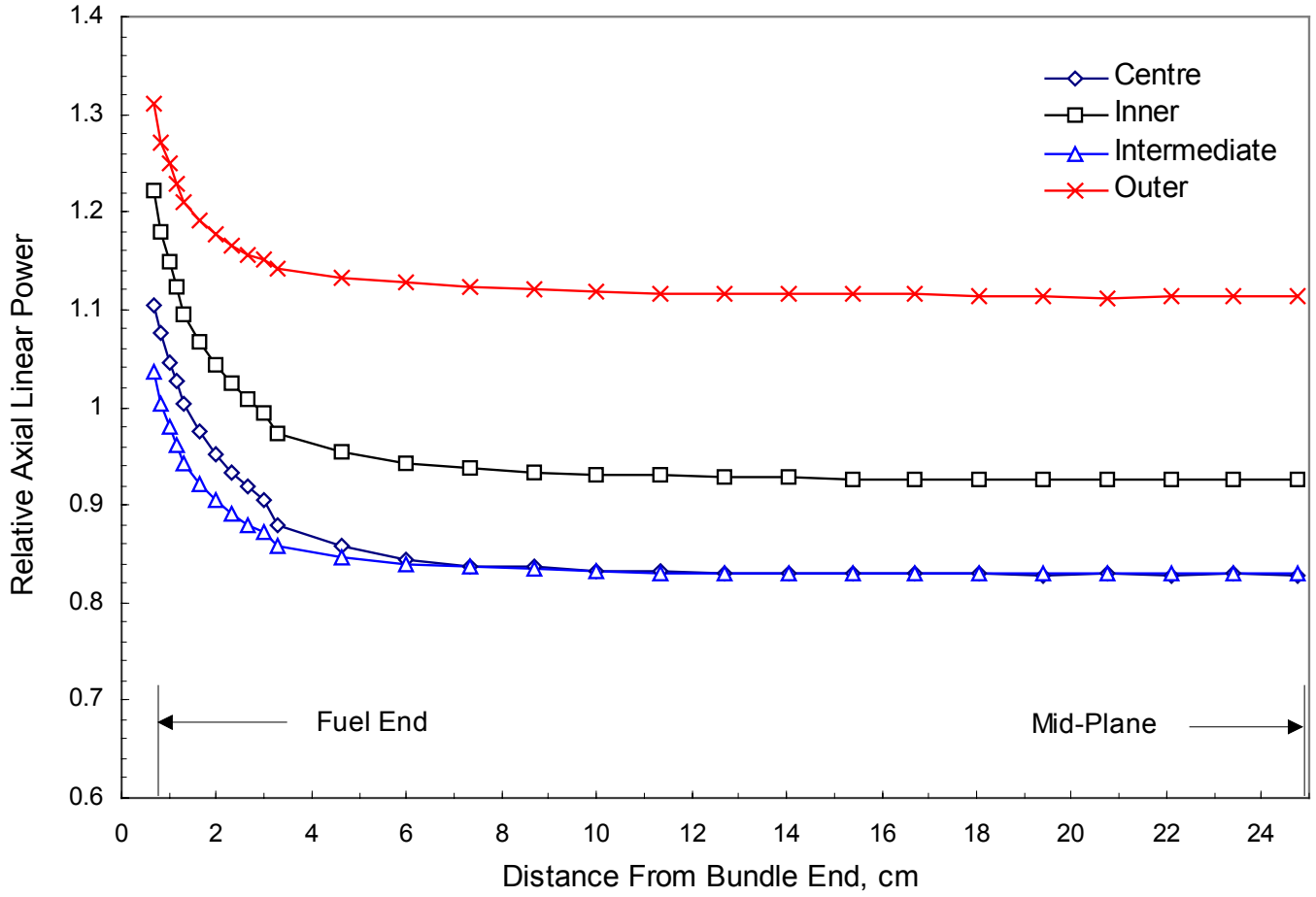

Figure 9: Relative Axial Linear Power Profile for Fresh CANDU NG CANFLEX-SEU Fuel, in Bundle-Bundle Contact Configuration (Bundle-Average Linear Power is Normalized to 1.0)

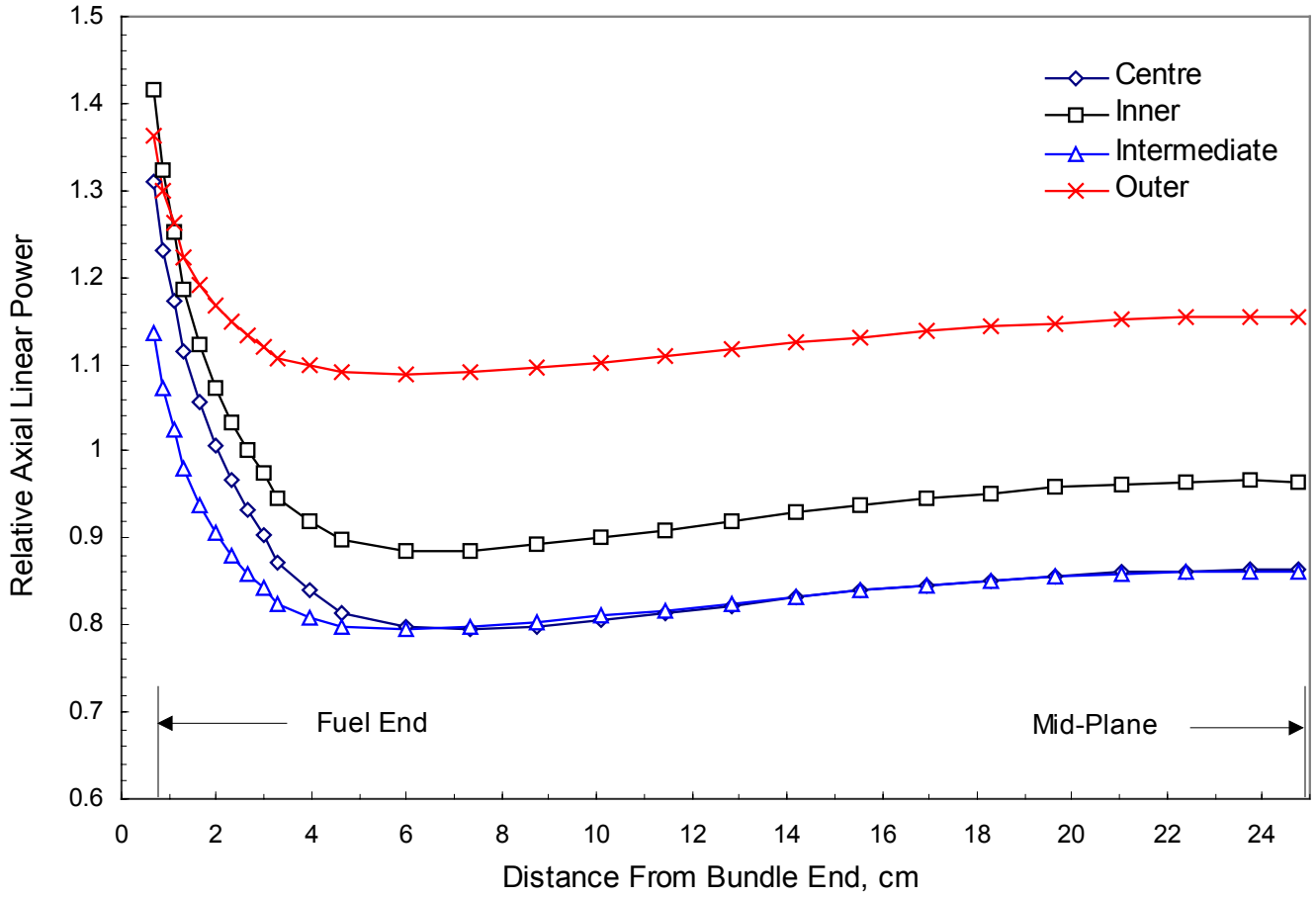

Figure 10: Relative Axial Linear Power Profile for Fresh CANDU NG CANFLEX-SEU Fuel, in Bundle-Coolant Contact Configuration (Bundle-Average Linear Power is Normalized to 1.0)